Reexamination of group velocities of structured light pulses

Peeter Saari*
Institute of Physics, University of Tartu, W. Ostwaldi 1, 50411 Tartu, Estonia
and Estonian Academy of Sciences, Kohtu 6, 10130 Tallinn, Estonia

(Received 21 March 2018; published 12 June 2018)

Recently, a series of theoretical and experimental papers on free-space propagation of pulsed Laguerre-Gaussian and Bessel beams was published, which reached contradictory and controversial results about group velocities of such pulses. Depending on the measurement scheme, the group velocity can be defined differently. We analyze how different versions of group velocity are related to the measurable travel time (time of flight) of the pulse between input (source) and output (detecting) planes. The analysis is tested on a theoretical model—the Bessel-Gauss pulse whose propagation path exhibits both subluminal and superluminal regions. Our main conclusion from resolving the contradictions in the literature is that different versions of group velocity are appropriate, depending on whether or not the beam is hollow and how the pulse is recorded in the output plane—integrally or with spatial resolution.

DOI: 10.1103/PhysRevA.97.063824

I. INTRODUCTION

Structured light fields, particularly the nondiffracting and twisted beams, are being increasingly used in different fields of research (see reviews [1–3]). Recently, a series of papers [4–13] was published, which deal with slower than c group velocities of pulses of these beams in free space and indicate promising applications of such subluminal light propagation.

In Ref. [4], using time-correlated photon pairs and a sophisticated measurement of propagation delays via the Hong-Ou-Mandel dip, the subluminality of photons in both a Bessel beam and in a focused Gaussian beam was shown. This paper garnered substantial coverage in the general media because the study purported to discover subluminal photons. Since, at least for the physical optics community, the observed phenomenon had been well known, the paper [4] encountered significant criticism. In particular, a comment [5] finds the interpretation of the results and the title of the paper misleading and states that the measurements only provide the projection of the photon velocity onto the axis of beam propagation. From our point of view, the most valuable contribution of Ref. [4] is a new concept of spatially averaged group velocity and its theoretical reasoning. As we will see below, although this new definition of group velocity corresponds well to a particular type of time-of-flight measurements of light pulses, it leads to a contradiction in the case of certain Bessel beam pulses.

The next theoretical paper [6] generalizes the concept of spatially averaged group velocity to Gaussian beams with orbital angular momentum (OAM). The same (twisted) beams were studied in Ref. [7], where curves of group velocity, calculated from the common (not spatially averaged) expression, were related to experimental data. However, our analysis [8] led to the conclusion that the results of [7] are questionable in several respects and, in particular, that when interpreting the measured relatively large propagation delays, one must not use the absolute value of the group velocity as done in [7], but, instead, its projections onto the beam axis. The very recent paper [9] shows that the group velocity obeys a relationship similar to one proposed 80 years ago by Majorana between spin and mass for relativistic particles. This paper also points out that what was measured in Refs. [4,7] as group velocity was, in fact, its projection onto the beam propagation axis.

In the theoretical paper [10], reduction of the group velocity (not spatially averaged) below the value c in the case of certain Bessel beam pulses has been considered. We pointed out in our critical comment [11] that the authors treat the problem as if only one type of Bessel pulse exists, no matter how it is generated, while it is well known from the literature that such pulses may be not only subluminal but superluminal as well.

The very recent study [12], which is a continuation of the work [4] and uses the same experimental technique, deals with the intrinsic delay introduced by "twisting" a photon. The authors reach the surprising result that the addition of OAM reduces the delay (i.e., makes the pulse somewhat faster) with respect to exactly the same beam with no OAM. Finally, a recent paper [13] analyzes theoretically how to set the group velocity of ultrashort light pulses in vacuum to arbitrary values within the focal region.

As distinct from focused beams, pulses of (pseudo)nondiffracting beams are propagation invariant, i.e., their intensity profile changes neither in any lateral nor in the axial direction over a large spatial range. Experimental realizability of the simplest type of such pulses, called the Bessel-X pulse, was demonstrated in [14], where we used the same optical scheme, with an annular slit, as Durnin *et al.* in their seminal work [15] on the Bessel beam. A narrow annular slit with angular radius θ ensures that the frequency-dependent phases of all Bessel beam constituents of the polychromatic field are proportional to the frequency: $z\cos\theta\,\omega/c$. The group velocity in this case is $c/\cos\theta$, i.e., superluminal, since it is given by the reciprocal of the mixed derivative of the phase

*peeter.saari@ut.ee

with respect to frequency and propagation coordinate z. There is massive literature on various nondiffracting pulsed waves (also called propagation-invariant localized waves) which are classified into superluminal, luminal, and subluminal types (see [3] and reviews [16–20]).

In a sense, the discussion of *subluminality* of structured light in the recent literature is *déjà vu*: in the preceding decade, the meaning of *superluminality* of nondiffracting pulses was intensively debated. Despite the experimental proofs [14,21,22], the feasibility of superluminal group velocities of Bessel-X-type pulses was questioned until we carried out direct measurements [23,24] of the spatiotemporal electric field of such pulses generated by a refractive axicon (conical lens).

In contradistinction to superluminal nondiffracting pulses generated by an annular-slit-and-lens scheme or a refractive or reflective axicon, the so-called pulsed Bessel beams generated by circular diffraction gratings—which are precisely what were considered in [4] and [10]—are always subluminal and are not propagation invariant because they spread temporally. This was shown theoretically a long time ago [25–27] and experimentally in [28,29] with femtosecond-range temporal and micrometer-range spatial resolution of the propagating field. A mistake in the mathematical derivation of group velocities, which led to the inability of some authors to distinguish the Bessel-X pulse from the pulsed Bessel beam and to accept the superluminality of the former, is analyzed in the review article [30].

In some forthcoming calculations, we resort to two-dimensional (2D) analogues of cylindrically symmetric 3D fields, i.e., to fields that depend—in addition to the longitudinal coordinate and time—on only one transverse coordinate. In expressions for such 2D fields, the zeroth-order Bessel function J_0 is replaced by a cosine. Propagation properties of 2D field pulses coincide, *mutatis mutandis*, with those of 3D ones. For a propagation-invariant nondiffracting pulse, the so-called focus wave mode which was theoretically intensively studied at the end of the previous century, this coincidence was shown in [31], where experimental feasibility of this exactly luminal wideband pulse had also been demonstrated. A general theory of 2D luminal and superluminal propagation-invariant (localized) waves was developed in [32]. Having in mind, e.g., the fast development of light-sheet microscopy and emerging applications of Airy beams, the 2D nondiffracting pulses cannot be considered as inferior to the 3D ones. A very recent article [33] demonstrates the generation of 2D nondiffracting pulses of different group velocities by means of a spatial light modulator.

For the forthcoming analysis, it is useful to recall that even the pulses of the fundamental Gaussian beam may exhibit both slightly superluminal and slightly subluminal propagation near their focus or the Rayleigh range [34–38]. The behavior of the group velocity of a polychromatic beam depends on the frequency dependence of the (interrelated) parameters of the monochromatic constituent beams, which in turn is determined by the optics generating the beam. On the basis of the character of the frequency dependence, pulses built from Gaussian, Bessel, Airy, etc. beams can be generally divided into different types [37,39–41], each possessing its own specific group-velocity properties.

If we juxtapose the recent papers [4–12] with the earlier literature referred to above, the following questions arise. How is the group velocity that is evaluated in an ordinary way related to the propagation time (time of flight) of the pulse between the input (source) and output (recording) planes? How does one take into account nonconstancy of the velocity over the propagation distance? Is the axial projection of the velocity or some other quantity appropriately related to the times or delays in flight, measured in experiments with hollow beams—such as the Laguerre-Gauss and other beams with OAM? And last but not least, how does one resolve the contradiction between the notion of the spatially averaged group velocity—which is always subluminal and was introduced in [4] for relating to time-of-flight experiments—and the superluminality of X-type nondiffracting pulses? The purpose of the present study is to give answers to these questions based on a model pulsed beam—the Bessel-Gauss pulse. This model pulse seems to be the most appropriate one for our purpose since it exhibits both superluminal and hollow-beam propagation stages and is physically realizable.

The paper is organized as follows. In the next section, different definitions of group velocities at off-axis field points are considered and the most suitable quantity for relating to the axial time of flight is chosen using a cylindrically symmetric Bessel-Gauss pulse [42–45] as a numerical test. Having in mind that the notion of group velocity generally describes well the propagation of narrowband pulses only, in Sec. III spatiotemporal evolution of an ultrashort Bessel-Gauss pulse with a particular wideband spectrum is calculated, resulting in a series of 3D plots. These plots can be considered as "snapshots in flight" of the pulse and they are analyzed in order to verify and to more deeply interpret the results of Sec. II. Finally, Sec. IV is devoted to solving the paradox that the formula of spatially averaged group velocity derived in [4], which supposedly is equal to the ratio of propagation distance and time, does not apply to superluminal pulses.

II. DIFFERENTLY DETERMINED GROUP VELOCITIES FOR EXAMPLE OF BESSEL-GAUSS PULSE

The well-known expression of the group velocity at a point $\mathbf{R}$ of a three-dimensional wave packet with the carrier (mean) frequency ω reads [46]

$$v(\mathbf{R}) = \frac{1}{|\nabla[\varphi'_\omega(\mathbf{R})]|}, \tag{1}$$

where $\varphi'_\omega(\mathbf{R})$ denotes the derivative of the spatial phase of the monochromatic constituents of the packet with respect to frequency. From an experimentalist's point of view, the observable quantity of primary interest is time τ that the pulse peak (or other feature) needs to travel from a certain starting (source) plane to the output (recording) plane. In the case of a plane-wave pulse or when the pulse peak propagates along a straight line—the optical axis z of a paraxial beam—it is not a problem to relate $v(\mathbf{R})$, the time τ, and the propagation depth $z = z_{\text{out}} - z_{\text{in}}$ with each other. But generally, even for paraxial beams, the quantity $v(\mathbf{R})$ is inappropriate for finding the travel time τ for a given propagation depth. For example, the intensity of a Laguerre-Gaussian beam is concentrated not on the axis but at a certain radial distance from it which increases as the pulse moves away from the focus. Due to the latter circumstance, as pointed out in [8], the pulse travel time τ is not determined

by $v(\mathbf{R})$, which is the magnitude of the group velocity vector, but rather by its projection onto the propagation axis z. Also, it should be stressed here that this z projection is generally not given by replacing the gradient operator in Eq. (1) with $\partial/\partial z$.

In order to propose such velocity quantities which are appropriate for relating to travel time versus propagation depth data from time-of-flight-type experiments, let us take one step back in the derivation of Eq. (1). As shown in [46], the instant of time at which the modulus of the field reaches its local maximum at position $\mathbf{R}$ is given by

$$\tau(\mathbf{R}) = \varphi'_\omega(\mathbf{R}). \tag{2}$$

If the pulse peak, i.e., its absolute maximum, passes through the point $\mathbf{R}$, the quantity $\varphi'_\omega(\mathbf{R})$ directly measures the time of flight of the pulse. For definiteness, let us choose the origin of the coordinate z so that the pulse peak passes through the plane $z = 0$ at the instant $t = 0$. Then, we can define an average group velocity in the direction of the optical axis over the distance z as follows:

$$v_a(z,r) = \frac{z}{\tau(z,r)}. \tag{3}$$

Here, we have introduced cylindrical coordinates (z,r,ϕ) for the point $\mathbf{R}$ and assumed that $\varphi'_\omega(\mathbf{R})$ does not depend on the azimuthal angle ϕ, which is true not only for beams with cylindrical symmetry but also for beams possessing orbital angular momentum, as long as the contribution of the azimuthal angle to the phase of their field does not depend on the frequency. In the supplemental material of Ref. [4], this velocity has been obtained by harmonic averaging of $v(\mathbf{R})$ over distance from z_1 to z_2 and used as an intermediate quantity in the derivation of a three-dimensionally averaged velocity, which we consider in Sec. IV.

The Born-Wolf velocity given by Eq. (1) in the cylindrical coordinates reads

$$v(z,r) = \frac{1}{\sqrt{\left[\frac{\partial}{\partial z}\tau(z,r)\right]^2 + \left[\frac{\partial}{\partial r}\tau(z,r)\right]^2}}. \tag{4}$$

As this quantity is the magnitude of the group-velocity vector which has been directed along $\nabla[\tau(z,r)]$, the projection of the group velocity onto the optical axis is obtained through multiplication by the directional cosine, resulting in

$$v_z(z,r) = \frac{\frac{\partial}{\partial z}\tau(z,r)}{\left[\frac{\partial}{\partial z}\tau(z,r)\right]^2 + \left[\frac{\partial}{\partial r}\tau(z,r)\right]^2}, \tag{5}$$

and, in the same way, the radial component of the velocity reads

$$v_r(z,r) = \frac{\frac{\partial}{\partial r}\tau(z,r)}{\left[\frac{\partial}{\partial z}\tau(z,r)\right]^2 + \left[\frac{\partial}{\partial r}\tau(z,r)\right]^2}. \tag{6}$$

In the case $\frac{\partial}{\partial r}\tau(z,r) = 0$, e.g., for on-axis points, the harmonic averaging of the axial group velocity $v_z(z,r)$ results in $v_a(z,r)$ defined by Eq. (3).

Figure 1 illustrates the differences between the quantities defined by Eqs. (3)–(5) in the case of an off-axis (hollow) diverging pulse.

Next, we calculate these velocities for a particular test field. As the latter, we have chosen a pulse of the Bessel-Gauss beam

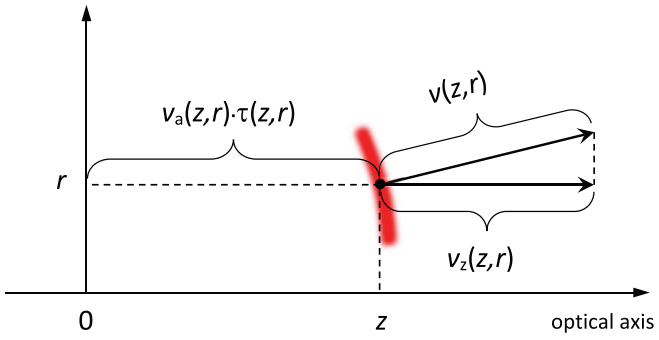

FIG. 1. Scheme of distinctions between the group velocities defined in the text.

since it is a paraxial, Gaussian-apertured, finite-energy and, hence, physically realizable version of the Bessel-X pulse. Moreover, it exhibits a pronounced and independently adjustable superluminality in the focal region, and in the far field its intensity is concentrated in a ring of diverging radius—quite similar to pulsed Laguerre-Gauss beams. The Bessel-Gauss beams—the monochromatic constituents of the pulse—are tractable as superpositions of Gaussian beams (modes), the optical axis of each of which lies along a generatrix of a cone. Half of the cone apex angle—which is called the axicon angle and typically designated by θ—determines the superluminal group velocity of the Bessel-X pulse as equal to $c/\cos\theta$ and, consequently, the same velocity for a pulse in the focal region of the Bessel-Gauss beam (henceforth the BG pulse).

It is known that the behavior of the group velocity in a pulsed Gaussian beam is determined by the frequency dependence of the (interrelated) parameters of the beam [34–37]. For example, if the Rayleigh range is inversely proportional to frequency, the on-axis group velocity is slightly superluminal in the focal region. The same holds for the Laguerre-Gauss beams [7]. Conversely, if the dependence is proportional to the frequency, the group velocity is slightly subluminal there. In order not to mix these effects on the group velocity with axicon-angle-controlled superluminality, we chose Gaussian beams whose Rayleigh range z_R is frequency independent to play the role of constituents of the BG pulse. Pulses formed from such beams—isodiffracting pulses—possess strictly luminal (equal to c) group velocity along the whole propagation axis [36,37]. Also, vanishing derivative $\partial z_R/\partial\omega$ keeps group-velocity expressions comparatively simple in the case of isodiffracting pulses.

According to [44], the monochromatic Bessel-Gauss wave function (without the time-dependent factor $\exp i\omega t$) of wave number $k = \omega c$ reads

$$\psi(z,r,k) = \frac{iz_R}{z+iz_R} J_0\left(\frac{iz_R}{z+iz_R}\theta kr\right) \times \exp\left\{-ik\left[\frac{r^2+z^2\theta^2}{2(z+iz_R)} + z\left(1-\frac{\theta^2}{2}\right)\right]\right\}, \tag{7}$$

where J_0 is the zeroth-order Bessel function of the first kind and θ is the axicon angle (apex half angle of a cone over the surface of which the directions of constituent Gaussian beams are evenly distributed). Equation (7) and Fig. 2 exhibit the

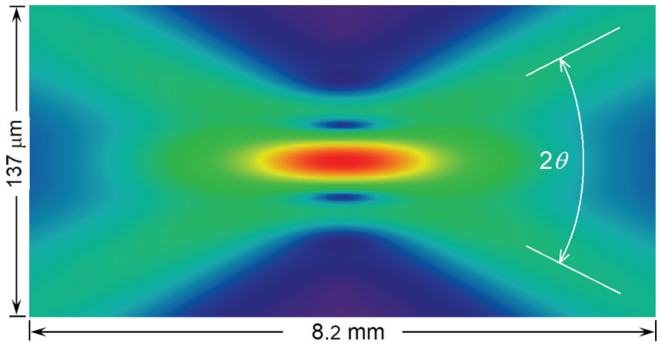

FIG. 2. Illustrative plot of a Bessel-Gauss beam. Depicted is the square root of the modulus of Eq. (7) without the first fraction. Note that the scale of the vertical axis representing the transverse coordinate $\pm r$ has been magnified 60 times relative to that of the z axis. Beam parameters: Rayleigh range $z_R = 3$ mm, wavelength $\lambda = 2\pi/k = 0.718$ μm, axicon angle $\theta = 1^\circ$, divergence of the constituent Gaussian beams $\theta_0 = (kz_R/2)^{-1/2} = 0.5^\circ$.

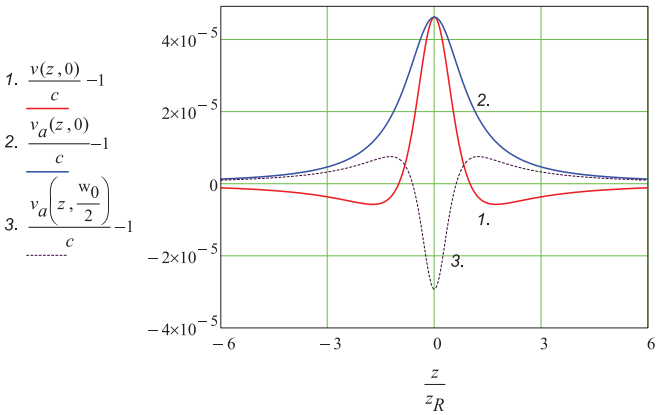

FIG. 3. Curves 1 and 2: on-axis group velocities defined by Eqs. (4) and (3), respectively, shown as normalized velocity changes vs the normalized propagation distance z. Curve 3: averaged group velocity along a line shifted radially from the z axis to half of the beam-waist radius $w_0 = 0.026$ mm or—in 3D terms—on the surface of a cylinder with radius $w_0/2 = 0.013$ mm. Beam parameters are the same as in Fig. 2, but the axicon angle $\theta = 0.55^\circ$ is smaller.

wave-function dependencies characteristic to both the Gaussian and Bessel beams.

The Gaussian radial profile suppresses the Bessel-function radial profile in the vicinity of the focal plane $z = 0$ and we see the side maxima of the Bessel function thanks to choosing the axicon angle twice larger than the divergence of the constituent Gaussian beams and taking the square root of the modulus (for improving contrast of the image). The spatial dependence of the field outside the focal region, i.e., where $|z| > z_R$, is seen with noticeable intensity thanks to omitting the factor $iz_R/(z + iz_R)$ in Eq. (7). This factor does not contribute to $\tau(z,r)$ according to Eq. (2) since z_R is frequency independent. The exponential factor contributes to $\varphi'_\omega(\mathbf{r})$ by the real part of the square brackets (divided by c since $\partial/\partial\omega = c^{-1}\partial/\partial k$). The derivative of the phase of the Bessel function can be evaluated via the identity

$$\frac{\partial}{\partial\omega}\arg U = \frac{1}{c}\,\mathrm{Im}\left(\frac{1}{U}\frac{\partial U}{\partial k}\right). \tag{8}$$

Expressing the derivative of the zeroth-order Bessel function through the first-order one and carrying out some algebra, we obtain

$$\tau(z,r) = \frac{z}{c} + \frac{1}{c}\frac{z\left(r^2 - \theta^2 z_R^2\right)}{2\left(z^2 + z_R^2\right)} + \frac{1}{c}\,\mathrm{Im}\left\{\frac{i\theta r z_R\, J_1\left(\frac{i\theta r z_R k}{z+iz_R}\right)}{(z+iz_R)\, J_0\left(\frac{i\theta r z_R k}{z+iz_R}\right)}\right\}, \tag{9}$$

where k now is the mean wave number of a quasimonochromatic wave packet. The first term on the right-hand side gives the arrival time at point z of a δ-shaped plane-wave pulse started from the origin $z = 0$ at $t = 0$. Hence, the following two terms are responsible for the temporal shift of the BG pulse relative to the "signal" pulse. It follows from Eq. (9) that everywhere on the axis z, the shift is negative since with $r = 0$ the third term vanishes. Negative temporal shift means superluminal group velocity. Indeed, as seen in Fig. 3, the average group velocity v_a ranges from the superluminal value $c/(1 - \theta^2/2) \simeq c/\cos\theta$ (which is the constant superluminal group velocity of the Bessel-X pulses) at the origin down to c at large propagation distances. This result was obtained earlier in [44], although without pointing out that this is the averaged group velocity, not the common local (Born-Wolf) group velocity v. In Fig. 3, the latter exhibits a transition to subluminal values as soon as the point exits from the Rayleigh range and reaches its minimum at $z = \pm\sqrt{3}\, z_R$, irrespective of the axicon angle θ. It is remarkable that the on-axis group velocity of such ordinary Gaussian pulsed beam, whose divergence θ_0 is frequency independent but the Rayleigh range is reciprocally proportional to frequency, behaves exactly the same way. A mathematical reason for this amazing coincidence is the identity of the expressions for $\tau(z,0)$ in both cases if one replaces the angle θ with θ_0. Physically, while the superluminality of the juxtaposed Gaussian beam pulse is caused by the frequency-dependent Gouy phase $\arctan(z/z_R)$, the superluminality of the BG pulse is a result of interference between its luminal Gaussian beam pulse constituents propagating under the axicon angle.

The third curve in Fig. 3 shows that while the averaged velocity is superluminal everywhere on the propagation axis, it turns out to be subluminal at off-axis points in the focal region. The Born-Wolf group velocity v along the same off-axis line is subluminal everywhere and exhibits two subluminal minima in the focal region—the curve being quite similar to that for the Laquerre-Gauss pulsed beam (Fig. 1 in [8]) and to curve 1 in Fig. 5 below.

Unless $\theta \ll \theta_0$, in other words, unless the BG pulse is almost like a Gaussian beam pulse, the on-axis and near-axis intensity is very low outside the Rayleigh range and therefore the curves in Fig. 3 are not of our main interest. According to our goals formulated in Sec. I, we must study the group-velocity behavior on the peak of the pulse. For the BG pulse, it means asymptotically along a generatrix of the cone, i.e., along the straight line $r = \theta\, z$; see Fig. 4 (being precise, the peak of the pulse transposes itself from the optical axis to the surface of the cone $r = \theta\, z$ when $z > z_R$, as we will see in the next section).

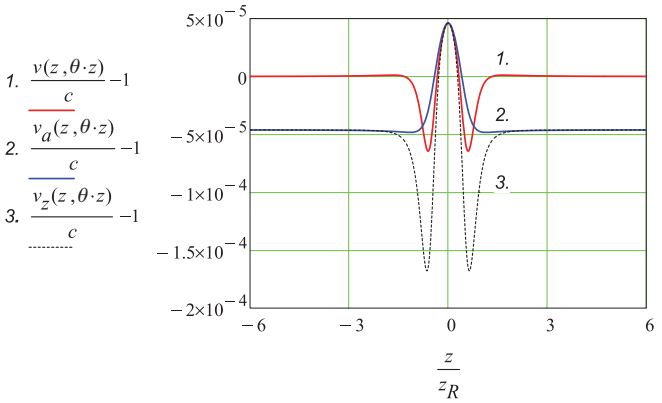

FIG. 4. Group velocities defined by Eqs. (4), (3), and (5) on the conical surface given by $r = \theta z$, plotted as functions of the propagation distance (curves 1, 2, and 3, respectively). Beam parameters are the same as in Fig. 3.

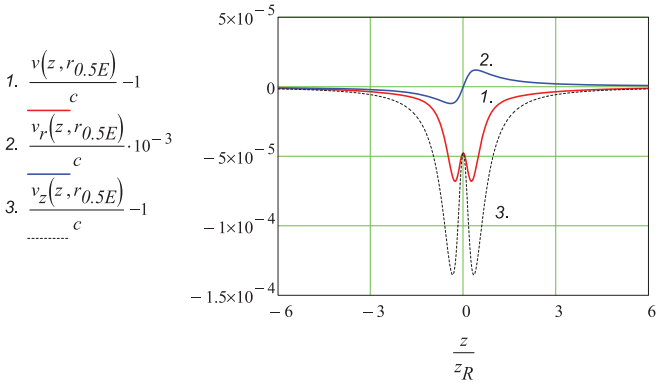

FIG. 5. Magnitude of the group-velocity vector and its radial and axial components (curves 1, 2, and 3, respectively) on the surface of a cylinder with radius $r_{0.5E} = 0.014$ mm $\approx w_0/2$. Beam parameters are the same as in Fig. 3. Note the scaling of v_r.

We see that the Born-Wolf group velocity is luminal everywhere in the Rayleigh range. This is understandable because at large distances the pulse peak area constitutes a converging (when $z < -z_R$) or diverging (when $z > z_R$) spherical zone and it is well known that the velocity of a spherical wave equals c. At the same time, since the group-velocity vector is directed under the axicon angle with respect to the z axis, its projection v_z to the propagation axis is *subluminal* everywhere in the Rayleigh range (as pointed out also in [8,9]). The same holds for the average group velocity v_a, which is directly related to the delays that are measurable experimentally. Asymptotically, $v_z \approx v_a \approx c\cos\theta$. Hence, in the case of pulses whose maximum does not propagate along the optical axis (Laguerre-Gauss pulsed beams and, alike, the BG pulse outside the Rayleigh range), if one studies the behavior of their group velocity via measuring their arrival delays in the far field, the results are determined by the subluminal plateau. It means that in a common experimental geometry, this plateau extends over distances much larger than the focal region where the velocity variations take place and, as a result, the variations remain masked in the delay data. In order to study the interesting behavior of the group velocity in the focal region, which distinctively depends on the type and parameters of the beam, in addition to the temporal resolution one must apply at least a submillimeter spatial resolution in the vicinity of the focus. This can be accomplished by the spatially encoded arrangement for temporal analysis by dispersing a pair of light E-fields (SEA TADPOLE) technique, as was done in Ref. [23]. These conclusions constitute one of the main results of the present study.

We point out that for plots in Figs. 3–5, the angles θ and θ_0 were taken almost equal. Changing the ratio θ/θ_0 reveals the following: (i) the region of the variable behavior of the velocities is confined by $\pm z_0$ rather than by $\pm z_R$, with z_0 being the z coordinate of the point where the line $r = \theta z$ attains the radial distance of the first zero of the Bessel profile; (ii) if $\theta/\theta_0 > 2$, the minima of v and especially of v_z become very deep in the vicinity of $\pm z_0$, while the radial component v_r acquires large values ($v_r > 0.5c$ when $\theta/\theta_0 > 3$) at these locations. Such steep variations start to manifest themselves also at the locations where the line reaches the radial distances of the next zeros of the Bessel profile. Although the beam intensity vanishes completely only on the rings corresponding to the zeros of the Bessel profile in the plane $z = 0$, at larger distances these zeros show up as intensity minima if $\theta/\theta_0 > 2$. Thus, the intensity minima cause the steep increase of the radial component v_r of the group velocity.

In order to comprehend the behavior of the radial component $v_r(z,r)$, we studied its z dependence at fixed nonzero values of r, and its r dependence at fixed nonzero values of z. Of course, $v_r(z,0)$ and $v_r(0,r)$ are identically equal to zero as follows from symmetry considerations already. Figure 5 shows the z dependence of the magnitude of the group velocity and its components on a cylindrical surface whose radius is equal to the HWHM of the pulse modulus at origin.

It follows from Fig. 5 that the plotted off-axis velocities v and v_z are subluminal everywhere and have obtained two minima (as is the case with the off-axis group velocity of Laguerre-Gauss beams [8]). Since the equality $v_z^2 + v_r^2 = v^2$ holds for any point, the minima coincide with the maxima of $|v_r|$. When $z < 0$, the beam converges and, therefore, $v_r < 0$ at that stage of the propagation of the pulse. At the diverging stage, the group-velocity vector has been directed away from the propagation axis, i.e., $v_r > 0$ when $z > 0$. However, there is a subtlety: at a fixed distance $0 < z \ll z_R$, the positive value of v_r grows steeply (up to $0.5c$) when r approaches the radial distance r_{01} of the first zero of the Bessel profile; then at the point r_{01} reverses the sign of its value and decreases to zero at the halfway to the radial distance r_{02} of the next zero, where the the same behavior repeats itself. Hence, figuratively speaking, the cylindrical surfaces with radii $r_{01}, r_{02}, \ldots$ attract the field flow and deflect the group-velocity vector in the vicinity of the focus.

In the next section, we correlate the obtained velocity curves with numerically simulated propagation of a wideband BG pulse whose duration and other parameters are suitable from an experimentalist's point of view. At the same time, we recall that the notion of group velocity assumes neglecting the higher than $\varphi'_\omega(\mathbf{R})$ derivatives of the spatial phase, which become significant with increasing bandwidth and are responsible for distortions of the pulse in the course of propagation.

III. PROPAGATION OF MODEL BESSEL-GAUSS PULSE WITH POISSON-LIKE SPECTRUM

For a better understanding of the results of the preceding section, it would be helpful to graphically depict the spatiotemporal evolution of a BG pulse. Porras [44] has found a suitable closed-form expression for the wave function of a BG pulse with the so-called Poisson-like spectrum $f(\omega) = \pi t_0^{n+1}\omega^n \exp(-\omega t_0)/n!$, where $\omega > 0$, $t_0 > 0$ determines the duration of the pulse, and n is a natural number. With somewhat changed designations, the expression reads

$$\Psi(z,r,t) = \frac{iz_R}{z+iz_R}\left\{\frac{it_0}{\sqrt{(t_c+it_0)^2-\left[\frac{iz_R}{c(z+iz_R)}\theta r\right]^2}}\right\}^{n+1} \times P_n\left\{\frac{t_c+it_0}{\sqrt{(t_c+it_0)^2-\left[\frac{iz_R}{c(z+iz_R)}\theta r\right]^2}}\right\}, \quad (10)$$

where $P_n()$ is the Legendre polynomial of the order n and

$$t_c = t - z(1-\theta^2/2)/c - \frac{1}{2c(z+iz_R)}(r^2+z^2\theta^2) \quad (11)$$

is a space-dependent complex time. As is well known, the group-delay and group-velocity expressions are, strictly speaking, meaningful if the FWHM $\Delta\omega$ of the pulses' spectrum is much smaller than its mean frequency ω_m. If this narrowband condition is not fulfilled, the pulse undergoes distortions in the course of propagation. On the other hand, a narrowband BG pulse would inevitably be too long for observation of the expected tiny differences of its propagation velocity from that of a plane wave, i.e., from c. Besides, since it follows from Eq. (10) that $\Delta\omega/\omega_m \sim 1/\sqrt{n}$, the narrowband condition would require a numerical evaluation of Legendre polynomials of very high order, which could cause computational problems. We have chosen $n = 16$ as this value corresponds roughly to $\Delta\omega/\omega_m \lesssim 1/2$ and gives a three-cycle pulse. Last but not least, temporal shifts as small as ≈ 1 fs of such ultrashort light pulses are easily observable with our interferometric setup based on a supercontinuum laser [29,41].

Evolution of the pulse in the course of propagation is shown in Fig. 6. The plots depict radial and temporal behavior of the pulse modulus in six cross-sectional planes with fixed values of z. A part of the profile seen to the left from the abscissa value $z/c - t = 0$ shows the temporal behavior of the modulus in every given z plane after the instant when a luminally propagating signal would cross the z plane (it is assumed that the "signal" starts when the peak of the pulse is at the position $z = 0$). Conversely, a part of the profile seen at the positive values of $z/c - t$ shows the temporal behavior of the modulus ahead of the signal. Such a representation of spatiotemporal evolution of ultrashort light pulses is common in femtosecond-resolution measurements that use the SEA TADPOLE technique. However, it is easier to comprehend the plots as "snapshots in flight" or "still frames" taken in the meridional plane of the beam at sequential fixed time instants. In the given case, the instants would be $t = 0$, $t = 834$ fs, $t = 1.6$ ps, $t = 3.3$ ps, $t = 6.7$ ps, and $t = 10$ ps (the values corresponding to $z = 0,\ 0.25, \ldots, 3$ mm) and the horizontal extent of each "frame" is 12.5 μm. Such an equivalence of the two representations is possible because the paraxial and ultrashort field practically does not change its shape when propagating over a distance as short as 12.5 μm during ≈ 40 fs. Indeed, to check the equivalence, we also calculated the plots from Eq. (10) with the fixed values of the variable t and it turned out that the values of the modulus in corresponding matrices (every element or pixel) of the two sets of plots are equal with accuracy $\leqslant 0.5\%$. In what follows, we refer to Fig. 6 as if it contains the "still frames."

The first frame depicts the instantaneous intensity profile (more exactly, its fourth root for better visibility of low-intensity features) of the BG pulse at the origin (in the focus of its Gaussian constituents). The X-like (actually a double conelike in 3D space) structure peculiar to the Bessel-X pulse [14,23] with some residual Bessel beam minima around the apex is clearly seen. We have intentionally chosen the axicon angle $\theta = 2^\circ$ larger than that in the plots of the previous section, i.e., four times exceeding the Gaussian divergence $\theta_0 = 0.5^\circ$, in order to reveal these minima and the wings of the pulse. The next two frames indicate that the pulse is superluminal—it outstrips a copropagating plane-wave reference whose sequential positions have been marked by the small white vertical bars. As distinct from the propagation invariance of the Bessel-X pulse, the BG pulse in the subsequent frames loses its double-conical shape with superluminal apex due to the limited (Gaussian) transversal dimension of the constituent beams. As a result, after reaching the Rayleigh range, the BG pulse peak intensities constitute a ring whose radius grows linearly with propagation distance. In other words, points of highest intensity move along the cone surface, the generatrix of which obeys the equation $r = \theta z$ used in plots of the preceding section. The last three frames show that the z-directed velocity of propagation of the ring is subluminal, thus indicating the reason for the subluminal plateau in Fig. 4.

Horizontal dashes in Fig. 6 mark values of r at which the line $r = \theta z$ intersects the frames. Note that the abscissa scale is stretched 20 times with respect to the r axis of the frames. This scale stretching explains why, in the last three frames, the pulse fronts are not practically vertical, i.e., perpendicular to the line $r = \theta z$ (as they should be in the case of equal scales).

The main conclusions from the plots of the pulse propagation are as follows.

(1) Group velocities are superluminal in the spatial region where the constituent Gaussian beam pulses, propagating along a pair of the cone generatrices of opposite inclination with respect to the z axis, overlap and interfere with each other. Note that the pulse profile in the first two frames resembles the Bessel-X pulse which is superluminal (the similarity of the Bessel-Gauss and Bessel-X fields has also been demonstrated in [44]).

(2) Outside this region—see the last two frames—the pulse propagates like a spherical zone and although the group-velocity vector in the peak of the pulse is directed along the generatrix and its magnitude is c, the projection of the peak position onto the z axis lags behind the luminal signal. Figure 4 indicates that this lag at large propagation depths $z \geqslant z_R$ results from subluminal values of v_a and v_z at the radius of the peak position, which both approach their far-field value $c\cos\theta$.

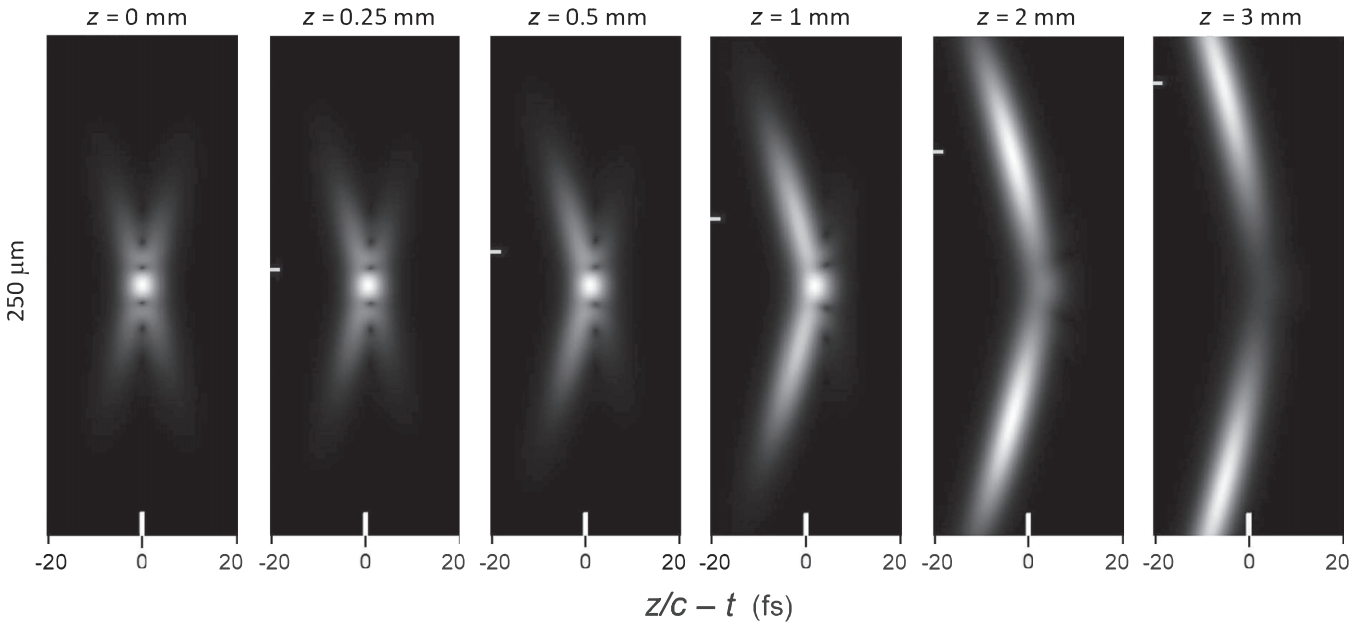

FIG. 6. Evolution of the modulus of the BG pulse plotted from Eq. (10) at sequential distances from the focus at $z = 0$. The vertical axis represents the transversal coordinate $\pm r$. The vertical white bars indicate the positions of $t = z/c$, i.e., the time instants that an ultrashort plane-wave pulse would reach the corresponding coordinate z if it copropagated along the z axis together with the BG pulse. The yellow horizontal dashes mark the radial distances $r = \theta z$. The parameters of the pulse are the axicon angle $\theta = 2^\circ$, the Rayleigh range $z_R = 3$ mm, $t_0 = 7$ fs ($ct_0 = 2$ μm), and $n = 16$. The frames have been normalized to unity (white). For a better revealing of the weak wings of the pulse, the grayscale has been taken proportional to $\sqrt{|\Psi(z,r,t)|}$.

(3) The two middle frames show that in the transition region, the superluminal apex dies out gradually while the intensity shifts to the spherical zone, resulting in the transition of v_a and v_z from superluminal to subluminal values, also seen in Fig. 4.

Hence, these conclusions are in accordance with the results of the preceding section, despite the fact that the group-velocity expressions used there are, in principle, determined for a quasimonochromatic pulse. Moreover, as shown in Appendix A, reshaping of the wideband pulse in the course of propagation is in agreement with Eq. (9) and the curves of group velocity obtained in the preceding section.

Thanks to the symmetry property of the field, $\Psi(-z,r,-t) = \Psi^*(z,r,t)$, and hence $|\Psi(-z,r,-t)| = |\Psi(z,r,t)|$, from Fig. 6 it is easy to comprehend the behavior of the pulse at negative times, i.e., when the pulse converges to the focus. In the mirrored interpretation, the rightmost frame in Fig. 6 represents the pulse at the earliest time instant $t = -10$ ps (or its crossing the plane $z = -3$ mm) and the leftmost frame corresponds now to the latest time instant $t = 0$ when the pulse has converged to the focus. Thus, the behavior of the pulse at negative times is the following: initially, near $z = -3$ mm, the BG pulse is given a head start relative to the reference (the plane-wave "signal" pulse); thereafter, when reaching $z \approx -1$ mm, due to its subluminality the BG pulse has lost the advantage and the signal catches up with it, and at $z \approx -0.5$ mm, the pulse's peak is clearly lagging behind the signal; in the final stage of the focusing, the situation reverses—due to its superluminal velocity, the BG pulse catches up with the signal when they both reach the focal plane $z = 0$. From an experimentalist's point of view, more convenient is a scheme where the pulse under study starts from a plane $z = z_{\rm in} < 0$ together with the plane-wave pulse. If thereafter the pulse arrival time is measured at point $r_{\rm out}$ in a plane $z = z_{\rm out} > 0$, the total time τ of its flight is obviously determined by the expression which follows from Eqs. (9) and (3), viz.,

$$\tau = \tau(|z_{\rm in}|,r_{\rm in}) + \tau(z_{\rm out},r_{\rm out}) = \frac{|z_{\rm in}|}{v_a(z_{\rm in},r_{\rm in})} + \frac{z_{\rm out}}{v_a(z_{\rm out},r_{\rm out})},$$

while the reference pulse needs, for traveling the same distance, a time interval $(|z_{\rm in}| + z_{\rm out})/c$. As a matter of fact, in an experiment, instead of travel times τ, it is convenient to measure delays with respect to the plane-wave signal pulse. In this case, the position $z_{\rm in}$ of the input (start) plane is where the delay is initially zero.

It is appropriate to add here that for a BG pulse with fixed geometrical parameters, the propagation depth (or temporal interval) where the pulse profile transforms from the double-conical (X-like in the meridional section) shape to the spherical zone is nearly independent from the number of cycles in the pulse. What increases with n (while ω_m is kept constant by correspondingly adjusting the parameter t_0) is the duration of the pulse only—"thickness" of its profile in the plots.

In conclusion, despite the fact that the plots in Fig. 6 have been calculated for an ultrawideband pulse, the features of propagation of the BG pulse that they show are in accordance with the group velocities defined and studied in Sec. II.

IV. SOLVING THE PARADOX OF SPATIALLY AVERAGED GROUP VELOCITY

The group velocity defined in [4]—let us call it the 3D averaged velocity—is averaged not only over a distance from z_1 (particularly, $z_1 = 0$) to z [see Eq. (3)], but also over the

beam cross section from the optical axis to infinity by using the transversal profile of the beam as a weighting function. As a result of such averaging, the effective group velocity is given by an expression which is always subluminal and holds for all paraxial beams,

$$v_{3D} = \frac{c}{1 + \frac{\langle \mathbf{k}_\perp^2 \rangle}{2k^2}}, \tag{12}$$

where $\langle \mathbf{k}_\perp^2 \rangle$ is the dispersion (variance) of the transverse wave vector in the beam. In the case of higher-order Gaussian beams, e.g., Laguerre-Gaussian beams, the quantity $\langle \mathbf{k}_\perp^2 \rangle$ grows with the indices of the beam [6].

The velocity v_{3D} is not only always less than c, but also it does not depend on the propagation distance. This is apparently in variation not only with the results of the preceding sections, but also with what is well known about group velocities of different types of Gaussian, etc. beams. For example, for both axicon-generated and circular-grating-generated Bessel beams, the transverse (radial) wave vector has a fixed (nondispersed) value $k_r = k \sin\theta$, but only the latter beam possesses a subluminal velocity in accordance with Eq. (12). For both of these beams, the group velocities do not depend on position and hence any averaging over the radial coordinate r must give a value equal to the on-axis velocity, which is subluminal in the case of grating-generated Bessel beams (or so-called pulsed Bessel beams) and superluminal for axicon-generated Bessel beams (or the Bessel-X pulses). This is easily seen from the following derivation which we will also use later on.

The requisite *harmonic* averaging of the velocity v_a reduces to arithmetic averaging of the delay given by Eq. (2) which, according to [4], can be carried out by the following expression for the delay:

$$\tau(z) = \frac{\partial}{c\partial k'} \left\{ \arg \left[\int \psi^*(z,r,k)\, \psi(z,r,k')\, dS \right] \right\}_{k'=k}, \tag{13}$$

where $dS = r dr\, d\phi$ is an element of the beam cross-section area and integration over ϕ gives a factor 2π due to the cylindrical symmetry. The integral over r is proportional to the orthogonality condition between Bessel functions and although it diverges if $k' = k$, it is a real quantity. Hence, the k'-dependent phase enters into Eq. (13) only from the phase exponent factor of the beams, which is equal to $\exp(iz\sqrt{k'^2 - k^2 \sin^2\theta})$ for the pulsed Bessel beam and to $\exp(izk'\cos\theta)$ for the Bessel-X pulse. Taking the derivative $\partial/\partial k'$ of the phases and using division like in Eq. (3), we reach a subluminal value $c\cos\theta$ of the 3D-averaged group velocity for the pulsed Bessel beam—which reduces to Eq. (12) in the paraxial limit—and to a superluminal value $c/\cos\theta$ for the Bessel-X pulse. In other words, we reach the well-known results [3,14,21–30]. Note that the transversal averaging has no effect on occasions when the phase of the wave function does not depend on the transversal coordinates irrespective of the intensity profile of the beam. This is not the case with the fundamental and higher-order Gaussian beams for which the velocity v_a becomes subluminal with increasing r even if it is superluminal on the optical axis. Since all Gaussian beams are solutions of the paraxial wave equation and also Eq. (12) follows from Eq. (13) in the paraxial limit [4], one may suspect that the paraxial approximation is a cause of the described discrepancy.

The BG pulse is a convenient object for studying the sources of the discrepancy because (i) as we saw in Sec. II, the superluminal values of $v_a(z,r)$ in the vicinity of the origin are replaced by subluminal values as r increases, and (ii) in the limit $z_R \to \infty$ or $\theta_0 \to 0$, the BG pulse transforms to the Bessel-X pulse. Unfortunately, for the integrals with the Bessel functions that we encounter in Eqs. (12) and (13), no closed-form expressions can be found in tables of integrals. Therefore, we carry out the study on a 2D analog of the BG pulse, which, however, possesses all the features essential here. The wave function of a monochromatic constituent of such a 2D pulse—we name it the cosine-Gaussian (CG) pulse—is a solution of the 2D paraxial equation and is identical to Eq. (7) if there r is replaced by a transversal coordinate x, the first fractional factor is put under the square root sign, and the Bessel functions are replaced by their 2D counterparts—sine and cosine function. Thus, the expression for the delay is similar to Eq. (9), viz.,

$$\tau(z,x) = \frac{z}{c} + \frac{1}{c}\frac{z\left(x^2 - \theta^2 z_R^2\right)}{2\left(z^2 + z_R^2\right)} + \frac{1}{c}\,\mathrm{Im}\left\{ \frac{i\theta r z_R \,\sin\left(\frac{i\theta r z_R k}{z + i z_R}\right)}{(z + i z_R)\,\cos\left(\frac{i\theta r z_R k}{z + i z_R}\right)} \right\}, \tag{14}$$

where θ now is not the axicon angle but designates the angle under which two 2D Gaussian beams are inclined with respect to the z axis (see Fig. 3 which now depicts the beam section in plane (z,x) at any value of the third coordinate y).

Harmonic averaging of the velocity v_a is, in other words, a cross-section averaging of the reciprocal velocity which—if normalized with respect to c—in the plane $z = 0$ reads

$$\frac{c}{v_a(0,x)} = \lim_{z\to 0} \frac{c\tau(z,x)}{z} = 1 - \frac{\theta^2}{2} + \frac{x^2}{2z_R^2} + \frac{\theta x \tan(\theta k x)}{z_R} + \frac{\theta^2 k x^2}{z_R \cos^2(\theta k x)}. \tag{15}$$

A limit of Eq. (15), $z_R \to \infty$, results in a superluminal value $v_a = c/(1 - \theta^2/2) \approx c/\cos\theta$, which is simply the group velocity of propagation of the interference pattern between two plane waves—the 2D counterpart of the Bessel beam.

The averaging can be carried out by the following integration:

$$\frac{c}{v_{aa}} = N^{-1} \int \psi^*(0,x,k) \frac{c}{v_a(0,x)} \psi(0,x,k)\, dx, \tag{16}$$

where the subscript aa stands for the two-dimensional averaging (along the z and x axes) and $N = \int \psi^*(0,x,k)\psi(0,x,k)\, dx$ is the normalization factor. The intensity of the beam in the given case reduces to

$$\psi^*(0,x,k)\psi(0,x,k) = \cos^2(\theta k x)\, \exp\left(-\frac{k x^2}{z_R}\right). \tag{17}$$

With the weighting function given by Eq. (17), the integration in Eq. (16) can be carried out by each term of Eq. (15) with the help of tables and/or a symbolic calculation software. The result is the following:

$$\frac{c}{v_{aa}} = 1 + \frac{\theta_0^2}{8} + \frac{\theta^2 \exp\left(\frac{\theta^2}{\theta_0^2}\right)}{4\cosh\left(\frac{\theta^2}{\theta_0^2}\right)}, \tag{18}$$

where we have replaced k and z_R with a more transparent parameter—the Gaussian beam divergence angle θ_0 according to the known relation $kz_R = 2/\theta_0^2$. It is immediately evident from Eq. (18) that the fully averaged group velocity of the CG pulse is *subluminal*. The second term is the contribution to the subluminality that comes from the divergence of the wave vectors of the plane-wave constituents of the Gaussian beam (in the case of a 3D Gaussian beam, this contribution is $\theta_0^2/4$ due to the two-times-larger number of the transversal dimensions). Even if we go to the limit of two plane waves in Eq. (18) by letting $\theta_0 \to 0$, the result $1 + \theta^2/2$ nevertheless corresponds to subluminal velocity $v_{aa} = c/(1 + \theta^2/2) \approx c\cos\theta$. The same results follow from the averaging procedures with the help of 2D versions of Eqs. (13) and (12).

If we *first* go to the limit of two plane waves—as we did above after Eq. (15)—and *thereafter* carry out the averaging by the integration, we obviously get the *superluminal* velocity $c/\cos\theta$. The mathematical reason for such contradiction is that taking a limit and an improper integral need not be interchangeable operations. The physical reason is that the Gaussian aperturing introduces a dependence of the group velocity v_a on a transverse coordinate and v_a generally decreases with the increase of the distance from the optical axis, as we saw above.

These conclusions can be readily generalized to the 3D case: despite the fact that in the focus the BG pulse is superluminal, its fully averaged group velocity is subluminal. In contrast, the group velocity of the Bessel-X pulse is superluminal irrespective of how large the averaging area is. In this regard, it is interesting to evaluate the maximum radius r_{sl} of such disk of averaging, at which the averaged velocity of the BG is still superluminal. For the parameters used in Sec. II (indicated in Fig. 3), with the help of numerical integration we obtained $r_{sl} \approx 0.68 w_0 = 17.8\ \mu$m. For experimental observation of the superluminality of the BG pulse, it means that the diameter of the acceptance area of the probing or detecting device must be smaller than $\sim 34\ \mu$m. This is not a problem when the tip of an optical fiber is used as a probe, in which case an order-of-magnitude-better resolution can be achieved [23,29]. The circle with $r_{sl} \approx 0.68 w_0$ in the focal plane cuts the beam at the level 10% of its peak intensity, i.e., it embraces the pulse central peak almost completely. Nevertheless, as shown in Appendix B, the contribution to the averaged velocity, which originates from all the infinite off-axis areas with $r > r_{sl}$, outweighs the superluminal contribution, resulting in a subluminal value of the averaged velocity v_{3D}, in accordance with Eq. (12).

The presented analysis does not say that the three-dimensionally averaged group velocity is somehow more proper than the mean velocity v_a defined by Eq. (3). Both are directly related to experimentally measurable propagation times or delays, but the first quantity is applicable if the pulse is recorded without any spatial resolution in a transverse plane and the second one if the dependence of the delay not only on the propagation depth but also on the transverse coordinates is measured.

V. CONCLUSIONS

Our general conclusion is that an answer to the question of which version of group velocity the pulse time of flight between two planes (which are perpendicular to the pulse propagation axis) is directly related to depends on how the pulse is registered.

If its intensity is measured not only with temporal but also with spatial resolution so that for the peak or any other local feature at point $\mathbf{R}$ of the pulse profile the travel time $\tau(\mathbf{R})$ between the two planes is recorded, then the travel distance divided by $\tau(\mathbf{R})$ results in the group velocity $v_a(\mathbf{R})$ of that feature in the direction of the optical axis averaged over the travel distance. This version of averaged group velocity may be subluminal, luminal, or superluminal. By varying the position of the output plane near the beam focus, a detailed picture of the behavior of group velocity in the focal region can be obtained. In the far field, the Bessel-Gauss pulse and, generally, pulses of Laguerre-Gauss and other hollow beams propagate like an expanding spherical zone and therefore their Born-Wolf group velocity [46] equals c, i.e., is luminal. But measuring the time of flight of the pulse peak in a usual optical scheme with the output (detecting) plane in the far field exhibits a subluminal propagation, no matter how the group velocities behave in the focal region of these beams. The reason is that outside the Rayleigh range, the velocity $v_a(\mathbf{R})$ as well as the projection of the Born-Wolf group-velocity vector onto the propagation axis reach their common subluminal constant value determined by beam divergence. If the pulse is registered as a whole in the output (detecting) plane without spatial resolution, then the travel distance divided by the travel time τ of the pulse results in the three-dimensionally averaged group velocity v_{3D} introduced in [4,6]. For paraxial pulsed beams, this velocity (i) does not depend on the position of the planes and (ii) is always subluminal. These properties are not in contradiction with studies of superluminally propagating Bessel-X-type nondiffracting pulses for two reasons:

(1) Their superluminality has been examined with spatial resolution in their cross-sectional plane, and

(2) any physically realizable Bessel-X-type pulse has a finite aperture like the Bessel-Gauss pulse has the Gaussian aperture, and therefore the cross-sectional averaging of the group velocity results in a subluminal value as shown here for the Bessel-Gauss pulse.

The results obtained here also hold in the case of single-photon pulses as far as spatiotemporal dependencies in photon wave functions are the same as in classical wave packets.

ACKNOWLEDGMENTS

This research has been supported by the Estonian Research Council through Grant No. PUT369. The author thanks Ioannis Besieris, Daniele Faccio, John Lekner, Miguel Porras, and Václav Potoček for fruitful discussions, as well as Heli Lukner, Peeter Piksarv, and Andreas Valdmann for their valuable comments on the manuscript.

APPENDIX A: SUBTLETIES OF PROPAGATION OF THE BG PULSE

A closer look at the first three frames of Fig. 6 reveals that the pulse's peak slightly lags behind the X-shape symmetry plane given by the zeros of the Bessel profile, but nevertheless it moves superluminally. At the same time, curve 3 in Fig. 3 tells us that the bottom of the pulse's peak should propagate up to $z \lesssim 3/4\ z_R$ subluminally and therefore its shape in frames 2–6 in Fig. 6 should gradually become distorted from an oval to a horseshoe shape like "⊃." A closer study of this discrepancy reveals that it is caused solely by the 3.6-fold difference of the axicon angles that we have chosen in the preceding and the current section for clarity of the plots. Indeed, with the value $\theta = 2^\circ$, curve 3 in Fig. 3 obtains a shape corresponding to superluminal values of the velocity v_a over the whole range of distances z. Vice versa, plotting, with the value $\theta = 0.55^\circ$, the first frames of Fig. 6 with high resolution in the region of the central peak, the brightness distribution gradually changes indeed to a horseshoe shape.

There is another subtlety seen in the first frame, viz., at larger radial distances than the Bessel profile zeros, there are two maxima (the "branches" of X shape), one of which moves through the plane $z = 0$ before the instant $t = 0$ and the other later. At the same time, Eq. (9) turns to zero at $z = 0$, irrespective of the radial coordinate, which means that the intensity at these radial distances should reach its peak values at $t = 0$, i.e., in the middle between the branches where actually the frame shows the lowest intensities. A contradiction? No, because, first of all, in the case of the quasimonochromatic limit assumed by the notion of group velocity and, consequently, by Eq. (9), the frame would be fulfilled with a Bessel beam whose temporal profile at all radial distances would peak at $t = 0$, $z = 0$, and the "X branching" (formation of the double-conical profile) would occur at very large radial distances $r_X \sim cT/2\theta$, where T is the duration of the pulse. Parenthetically, r_X would encircle as many Bessel profile zeros, as many cycles the pulse contains. Moreover, there is no contradiction with Eq. (9) even in the case of the branches of the ultrawideband pulse in Fig. 6. Namely, if one plots from Eq. (9) the temporal shift $z/c - \tau$ (for $r = r_X$ evaluated from the pulse parameters of Fig. 6) as a function of z, one gets a curve which with increasing z immediately after the origin $z = +0$ jumps to negative values and then, in the vicinity of the point $z \approx 0.5 z_R$, turns to positive values. This is in accordance with the behavior we see in Fig. 6 also. Indeed, when the pulse center has passed the plane $z = 0$, the branches are no longer of equal intensity, the field modulus at $r = r_X$ has it maximum on the rear cone, and, since this cone moves behind the apex, the temporal shift is negative. With increasing z, however, since the whole double-conical part of the pulse profile moves superluminally, the beginning point of the rear (left) branch at $r = r_X$ gradually recovers from its initial lag and for it the shift $z/c - \tau$ becomes positive (note that here we are looking upon propagation of intensity or modulus maxima at a fixed radial distance from the z axis and not the propagation of the absolute intensity maximum of the pulse).

APPENDIX B: SUPER- AND SUBLUMINAL CONTRIBUTIONS TO THE 3D-AVERAGED VELOCITY

Here we evaluate how much power (intensity integrated over area) the disk with radius r_{sl} transmits in comparison to the total power (intensity integrated over whole plane $z = 0$) at the instant $t = 0$. Concerning the evaluation of the improper integral for the latter quantity, a numerical calculation would have been dubious because the integrand contains infinitely many times the oscillating Bessel function; see Eq. (7). Fortunately, we found a table integral given by Eq. (6.633.4) in Ref. [47] which readily gave an exact result:

$$\begin{aligned}\int_0^\infty \psi^*(0,r,k)\psi(0,r,k) r\,dr &= \int_0^\infty e^{-\frac{kr^2}{z_R}} J_0^2(\theta k r) r\,dr \\ &= k^{-1} z_R I_0(\theta^2 k z_R) \exp(-\theta^2 k z_R), \end{aligned} \tag{B1}$$

where $I_0(\cdot)$ is the modified Bessel function of the zeroth order. With the help of Eq. (B1), we found that in the case of the BG pulse, with the given beam parameters, as much as about 70% of the total power is embraced within the superluminality circle of radius r_{sl}. We conclude that the subluminal contribution to the averaged velocity, which originates from the 30% of the total power flowing in the off-axis area with $r > r_{sl}$, outweighs the superluminal contribution, resulting in a subluminal value of the averaged velocity, v_{3D}.

[1] H. Rubinsztein-Dunlop *et al.*, Roadmap on structured light, J. Opt. **19**, 013001 (2017).

[2] M. J. Padgett, Orbital angular momentum 25 years on, Opt. Express **25**, 11265 (2017).

[3] *Non-Diffracting Waves*, edited by H. E. Hernandez-Figueroa, E. Recami, and M. Zamboni-Rached (Wiley, New York, 2013).

[4] D. Giovannini, J. Romero, V. Potoček, G. Ferenczi, F. Speirits, S. M. Barnett, D. Faccio, and M. J. Padgett, Spatially structured photons that travel in free space slower than the speed of light, Science **347**, 857 (2015).

[5] Z. L. Horváth and B. Major, Comment on "Spatially structured photons that travel in free space slower than the speed of light," arXiv:1504.06059.

[6] N. D. Bareza and N. Hermosa, Subluminal group velocity and dispersion of Laguerre-Gauss beams in free space, Sci. Rep. **6**, 26842 (2016).

[7] F. Bouchard, J. Harris, H. Mand, R. W. Boyd, and E. Karimi, Observation of subluminal twisted light in vacuum, Optica **3**, 351 (2016).

[8] P. Saari, Observation of subluminal twisted light in vacuum: Comment, Optica **4**, 204 (2017).

[9] F. Tamburini and B. Thidé, Majorana states for apparently slow vortex photons in vacuum, arXiv:1707.07160.

[10] R. R. Alfano, and D. A. Nolan, Slowing of Bessel light beam group velocity, Opt. Commun. **361**, 25 (2016).

[11] P. Saari, Comments on "Slowing of Bessel light beam group velocity," Opt. Commun. **392**, 300 (2017).

[12] T. Roger, A. Lyons, N. Westerberg, S. Vezzoli, C. Maitland, J. Leach, M. Padgett, and D. Faccio, How fast is a twisted photon?, Optica **5**, 682 (2018).

[13] A. Sainte-Marie, O. Gobert, and F. Quéré, Controlling the velocity of ultrashort light pulses in vacuum through spatio-temporal couplings, Optica **4**, 1298 (2017).

[14] P. Saari and K. Reivelt, Evidence of X-Shaped Propagation-Invariant Localized Light Waves, Phys. Rev. Lett. **79**, 4135 (1997).

[15] J. Durnin, J. J. Miceli, Jr., and J. H. Eberly, Diffraction-Free Beams, Phys. Rev. Lett. **58**, 1499 (1987).

[16] R. Donnelly, and R. Ziolkowski, Designing localized waves, Proc. R. Soc. London A **440**, 541 (1993).

[17] I. Besieris, M. Abdel-Rahman, A. Shaarawi, and A. Chatzipetros, Two fundamental representations of localized pulse solutions to the scalar wave equation, Prog. Electromagn. Res. **19**, 1 (1998).

[18] J. Salo, J. Fagerholm, A. T. Friberg, and M. M. Salomaa, Unified description of nondiffracting X and Y waves, Phys. Rev. E **62**, 4261 (2000).

[19] P. Saari and K. Reivelt, Generation and classification of localized waves by Lorentz transformations in Fourier space, Phys. Rev. E **69**, 036612 (2004).

[20] A. P. Kiselev, Localized light waves: Paraxial and exact solutions of the wave equation (A review), Opt. Spectrosc. **102**, 603 (2007).

[21] I. Alexeev, K. Y. Kim, and H. M. Milchberg, Measurement of the Superluminal Group Velocity of an Ultrashort Bessel Beam Pulse, Phys. Rev. Lett. **88**, 073901 (2002).

[22] R. Grunwald, V. Kebbel, U. Griebner, U. Neumann, A. Kummrow, M. Rini, E. T. J. Nibbering, M. Piché, G. Rousseau, and M. Fortin, Generation and characterization of spatially and temporally localized few-cycle optical wave packets, Phys. Rev. A **67**, 063820 (2003).

[23] P. Bowlan, H. Valtna-Lukner, M. Lõhmus, P. Piksarv, P. Saari, and R. Trebino, Measurement of the spatio-temporal field of ultrashort Bessel-X pulses, Opt. Lett. **34**, 2276 (2009).

[24] P. Bowlan, H. Valtna-Lukner, M. Lõhmus, P. Piksarv, P. Saari, and R. Trebino, Measurement of the spatiotemporal electric field of ultrashort superluminal Bessel-X pulses, Opt. Photon. News **20**, 42 (2009).

[25] Z. Y. Liu, D. Y. Fan, Propagation of pulsed zeroth-order Bessel beams, J. Mod. Opt. **45**, 17 (1998).

[26] A. Shaarawi and I. M. Besieris, On the superluminal propagation of X-shaped localized waves, J. Phys. A: Math. Gen. **33**, 7227 (2000).

[27] M. A. Porras, Diffraction effects in few-cycle optical pulses, Phys. Rev. E **65**, 026606 (2002).

[28] M. Lõhmus, P. Bowlan, P. Piksarv, H. Valtna-Lukner, R. Trebino, and P. Saari, Diffraction of ultrashort optical pulses from circularly symmetric binary phase gratings, Opt. Lett. **37**, 1238 (2012).

[29] P. Piksarv, H. Valtna-Lukner, A. Valdman, M. Lõhmus, R. Matt, and P. Saari, Temporal focusing of ultrashort pulsed Bessel beams into Airy-Bessel light bullets, Opt. Express **20**, 17220 (2012).

[30] P. Saari, X-type waves in ultrafast optics, in [3], p. 109.

[31] K. Reivelt and P. Saari, Experimental demonstration of realizability of optical focus wave modes, Phys. Rev. E **66**, 056611 (2002).

[32] I. M. Besieris and A. M. Shaarawi, (2+1)-dimensional X-shaped localized waves, Phys. Rev. E **72**, 056612 (2005).

[33] H. E. Kondakci and A. F. Abouraddy, Diffraction-free space–time light sheets, Nat. Photon. **11**, 733 (2017).

[34] Z. Horváth, J. Vinkó, Z. Bor, and D. Von der Linde, Acceleration of femtosecond pulses to superluminal velocities by Gouy phase shift, Appl. Phys. B **63**, 481 (1996).

[35] Z. L. Horváth and Zs. Bor, Reshaping of femtosecond pulses by the Gouy phase shift, Phys. Rev. E **60**, 2337 (1999).

[36] S. Feng and H. G. Winful, Spatiotemporal structure of isodiffracting ultrashort electromagnetic pulses, Phys. Rev. E **61**, 862 (2000).

[37] P. Saari, Relativistic Doppler effect, aberration and Gouy effect on localized waves, Atti della Fondazione Giorgio Ronchi **58**, 729 (2003).

[38] M. A. Porras, I. Gonzalo, and A. Mondello, Pulsed light beams in vacuum with superluminal and negative group velocities, Phys. Rev. E **67**, 066604 (2003).

[39] C. J. R. Sheppard, Bessel pulse beams and focus wave modes, J. Opt. Soc. Am. A **18**, 2594 (2001).

[40] P. Saari, Laterally accelerating Airy pulses, Opt. Express **16**, 10303 (2008).

[41] A. Valdmann, P. Piksarv, H. Valtna-Lukner, and P. Saari, Realization of laterally nondispersing ultrabroadband Airy pulses, Opt. Lett. **39**, 1877 (2014).

[42] F. Gori, G. Guattari, and C. Padovani, Bessel-Gauss, Opt. Commun. **64**, 491 (1987).

[43] P. L. Overfelt, Bessel-Gauss pulses, Phys. Rev. A **44**, 3941 (1991).

[44] M. A. Porras, R. Borghi, and M. Santarsiero, Few-optical-cycle Bessel-Gauss pulsed beams in free space, Phys. Rev. E **62**, 5729 (2000).

[45] K. Reivelt and P. Saari, Bessel-Gauss pulse as an appropriate mathematical model for optically realizable localized waves, Opt. Lett. **29**, 1176 (2004).

[46] M. Born and E. Wolf, *Principles of Optics* (Pergamon, Oxford, 1975).

[47] I. S. Gradshteyn and I. M. Ryzhik, *Integrals, Series and Products*, 6th ed. (Academic, New York, 2000).